Electronic Supplementary Information for:

Novel dual near-infrared fluorescent probe for bioimaging and visualization of viscosity in acute alcoholic liver injury

Ruonan Wang,‡[a] Xucong Zhou,‡[a] Bingxue Li,‡[a] Ru Ding,[a] Jingqian Han,[a] Ying Wang,*[b,c] Aixia Meng[a] and Jin Zhou*[a]

[a.] *School of Pharmacy, School of Nursing, School of Basic Medical Sciences, Shandong Second Medical University, Weifang 261053, China*

[b.] *Faculty of Education, Qufu Normal University, Qufu 273165, China*

[c.] *School of Health and Life Sciences, University of Health and Rehabilitation Sciences, Qingdao 266071, China*

Corresponding Author

**E-mail: zhoujin@wfmc.edu.cn; wangying@uor.edu.cn.*

Table of contents

1. Experimental

Materials and Reagents. Aminobenzenethiol and IR-775 were purchased from Tixiay (Shanghai) Chemical Industry Development Co. N, N-dimethylaniline and trifluoroacetic acid were purchased from Sain Chemical (Shanghai) Co. Glycerol was purchased from Yantai Chemical Industry Research Institute (China). Tetrahydrofuran (THF), dichloromethane (DCM), N, N-dimethylformamide (DMF) and dimethyl sulfoxide were purchased from Yantai Far East Fine Chemical Co. Acetone, acetonitrile and ethanol were purchased from Sinopharm Chemical Reagent Co. Methanol was purchased from Tianjin Kemi Chemical Reagent Co. Dulbecco, Modified Eagle Medium (DMEM basic 1×) medium, phosphate buffered saline (PBS), penicillin and streptomycin were purchased from Solabio. Fetal bovine serum was purchased from Zhejiang Tianhang Biotechnology Co. 3-(4,5-dimethylthiazol-2-yl)-2,5-diphenyltetrazolium bromide (MTT) was purchased from Sigma-life Sciences. Dimethyl sulfoxide (cell grade) was purchased from Sain Chemical Technology (Shanghai) Co. Lipopolysaccharide was purchased from Shanghai Titan Technology Co. Nystatin was purchased from Aladdin Reagent (Shanghai) Co. Oleic acid was purchased from Sain Chemical Technology (Shanghai) Co. Dexamethasone was purchased from Shandong Zhengmu Biological Co. Chinese liquor was purchased from Beijing Red Star Co. All other chemical reagents were of analytical grade. Ultrapure water purified in Milli-Q reference system (Millipore) experiment.

Characterization Methods. ^{1}H NMR and ^{13}C NMR spectra were measured on a Bruker Avance NEO 400 MHz spectrometer. High-resolution electrospray ionization mass spectrometry (HR-ESI-MS) was measured on a Thermoscience Q extractor (Bremen, Germany).

Fluorescence spectra were measured by a prismatic spectrophotometer (F98 fluorescence spectrophotometer) in Shanghai, China. UV absorption spectra were measured using a Puxi Beijing spectrophotometer (T10CS spectrophotometer), China. An FE 20 pH meter (Mettler Toledo) was used. MTT cytotoxicity assay was performed using a multifunctional aldolase labeling method (Molecular Devices MTT M5, USA). Fluorescence images of cells were obtained using a CellInsight CX7 LZR high content analysis (HCA) platform (Thermo Fisher Scientific, Waltham, MA, USA) with a 40× objective. *In vivo* and *ex vivo* imaging was obtained by IVIS spectroscopy.

Synthesis of Probe. A synthetic route for **Cy-ND** was depicted in Scheme 1.

Cy-NH$_2$: the mixture of 3-aminothiophenol (60 mg, 0.48 mmol) and NaH (7 mg, 0.3 mmol) in a flask containing DMF (5 mL) was stirred under nitrogen atmosphere at room temperature for 15 min. Then, a solution of IR-775 (96.8 mg, 0.16 mmol) in DMF (1 mL) was added to the mixture using a syringe and the reaction mixture was heated at 55 °C for 12 h. After the reaction was cooled down to room temperature, organic layer was evaporated under vacuum. Then the crude product was separated by silica gel column chromatography with CH_2Cl_2/MeOH (100:1 to 10:1). The desired product was obtained as a blue-green solid (28 mg, 0.07 mmol, 45.0 %). Molecular formula: $C_{26}H_{27}N_2S^+$. The ^{1}H NMR, ^{13}C NMR and HR-MS spectra of probe **Cy-NH$_2$** are shown in the last part of Supporting Information respectively. ^{1}H NMR (400 MHz, DMSO-d6) δ 8.15 (d, J = 13.9 Hz, 1H), 7.69 (d, J = 7.4 Hz, 1H), 7.54 (d, J = 7.9 Hz, 1H), 7.48 (t, J = 7.4, 3H), 7.37 (t, J = 8.2 Hz, 1H), 6.90 (s, 1H), 6.80 (d, J = 8.6 Hz, 1H), 6.68 (s, 2H), 6.43 (d, J = 14.0 Hz, 1H), 3.75 (s, 3H), 2.73 (s, 2H), 2.67 (s, 2H), 1.83 (s, 2H), 1.71 (s, 6H). ^{13}C NMR (125 MHz, $CDCl_3$) δ 101.24, 96.14, 95.02, 94.59, 93.68, 93.25, 92.39, 91.55, 90.44, 90.11,

89.22, 88.47, 86.89, 86.05, 85.56, 83.31, 71.21, 70.12, 65.72, 65.02, 64.76, 64.41, 63.45, 63.02, 60.63. ESI HRMS (m/z): calcd for $C_{26}H_{27}N_2S$ $[M]^+$: 399.1889, found: 399.1889.

Cy-ND: the mixture of **Cy-NH₂** (23.0 mg, 0.057 mmol), $NaNO_2$ (8 mg, 0.12 mmol), amidosulfonic acid (12 mg, 0.12 mmol) and in CH_3CN/CH_2Cl_2/TFA (v/v/v, 1/4/0.01, 5 mL) at room temperature under N_2 atmosphere, was added and the solution was stirred for 20 min. Subsequently, N, N-dimethylaniline (46 μL, 361 μmol) dissolved in CH_3CN (1 mL) was added to the reaction mixture and the solution was stirred at 0 °C under N_2 atmosphere for 1 h. After completion of the reaction, the mixture was poured into water and extracted with dichloromethane. Then the organic phase was separated, dried with anhydrous Na_2SO_4 and concentrated under reduced pressure. The crude product was separated by column chromatography using CH_2Cl_2/MeOH (100:1 to 10:1) was subjected to silica column chromatography to purify the green solid (21.9 mg, 0.0412 mmol, 58.2%). Molecular formula: $C_{34}H_{35}N_4S^+$. The ^1H NMR, ^{13}C NMR and HR-MS spectra of probe **Cy-ND** are shown in the last part of Supporting Information respectively. ^1H NMR (400 MHz, $CDCl_3$) δ 8.35 (d, J = 14.4 Hz, 1H), 7.90 (t, J = 10.0 Hz, 3H), 7.83 (s, 1H), 7.54 – 7.49 (m, 4H), 7.46 – 7.43 (m, 2H), 7.11 (d, J = 14.5 Hz, 1H), 7.05 (s, 1H), 6.77 (d, J = 8.6 Hz, 2H), 4.24 (s, 3H), 3.14 (s, 6H), 2.90 (s, 2H), 2.78 (s, 2H), 1.99 (s, 2H), 1.81 (s, 6H). ^{13}C NMR (151 MHz, CD_3OD) δ 158.12, 153.68, 144.06, 143.93, 142.73, 141.29, 139.70, 134.66, 131.42, 129.74, 127.10, 126.63, 126.46, 126.34, 123.42, 123.20, 117.99, 112.56, 111.91, 108.21, 102.85, 33.26, 32.12, 31.75, 28.75, 28.17, 28.16, 28.10, 27.48, 27.48, 26.42, 21.92. ESI HRMS (m/z): calcd for $C_{34}H_{35}N_4S[M]^+$: 531.2577, found: 531.2581.

Theoretical Calculation. The Gaussian 16 A.03 program was used to perform theoretical calculations with the density-functional theory (DFT) and time-dependent density functional theory (TDDFT). The functional and basis set used were B3LYP-D3(BJ)/6-31G(d). To simulate a high degree of realism of **Cy-ND** in the water solution, the solvation model based on the integral equation formalism variant of the polarizable continuum model (IEFPCM) was utilized.

We have added the relationship between dihedral angle and transmission energy as shown in Fig. S9. We found that with the increase of the dihedral angle, the ground state energy increases gradually, and the excited state energy decreases gradually. When the dihedral angle is 94.36°, the excited state energy is at the minimum value, which means that the molecule is in the orthogonal configuration.

In addition, in order to help readers better understand, we have done the analysis of hole-electron distribution[1], which is a highly effective research method that accurately captures the behavioral characteristics of excited state electrons. To gain a deeper understanding of the TICT mechanism underlying electronic excitation, we employed the Multiwfn program[2] and VMD software[3] to meticulously create hole-electron distribution maps and C_{hole}-C_{ele} function diagrams, as depicted in Fig. S10. The green regions in the figure represent the distribution of electrons, while the blue regions reveal the distribution of holes. Fundamentally, electronic excitation involves the migration of electrons from holes. In the C_{hole}-C_{ele} function diagram, the blue and green spheres represent the centers of mass for holes (C_{hole}) and electrons (C_{ele}), respectively, visually illustrating the direction of charge transfer within the molecule.

Observing Fig. S10, it becomes evident that during the excitation process, electrons move from the dimethylaniline moiety to the sulfur-substituted hemicyanine dyes. Additionally, we

calculated relevant parameters associated with the hole-electron distribution, as summarized in Table S3. These data indicate that the hole-electron centroid distances (D) for **Cy-ND** with the dihedral angle of N18-N19-C20-C22 at 30°, 60°, 90° are 5.653, 7.318, and 7.618 Å, respectively, and all values exceed 5 Å, firmly establishing that the type of electronic excitation is charge transfer excitation. Furthermore, the hole-electron distribution values (S_r) for the three dihedral angles are 0.52383, 0.39630, and 0.14600 a.u., respectively, reflecting the overlap between holes and electrons gradually decreases as the dihedral angles gradually increases. It is noteworthy that the separation degree (*t*) between holes and electrons is positive, indicating that their separation becomes more pronounced. Changes in the hole delocalization index (*HDI*) and electron delocalization index (*EDI*) also support this trend. The above data fully show that **Cy-ND** has a TICT effect.

General Procedure for Spectroscopic Detection. Without other noted, all spectral properties test experiments are carried out in accordance with the following procedures. A stock solution (1.0 mM) of **Cy-ND** was prepared in DMSO. Water and glycerol were mixed into different proportions, the viscosity value that the experiments used were identical to the one used in the article reported earlier.[4] The solutions of **Cy-ND** of different viscosity were prepared by adding the stock solution (1.0 mM) 10 μL to 1 mL of solvent mixture (water-glycerol solvent systems) to obtain the final concentration of the probe **Cy-ND** (10 μM). The fluorescence emission was measured at λ_{ex} = 766 nm. All fluorescence measurements were conducted on a Shanghai F98 Fluorescence Spectrophotometer.

Selectivity Evaluation. Metal ions (Ca^{2+}, K^{+}, Mg^{2+}, Cu^{2+}, Cr^{3+}, Ni^{+}, Hg^{2+}, Pb^{2+}, Ag^{+}), glutathione (GSH) , amino acids (tyrosine (Tyr), cysteine (Cys), homocysteine (Hcy), serine

(Ser), alanine (Ala)), HSO_3^-, enzymes (nitroreductase (NTR), chymotrypsin, acetaldehyde dehydrogenase (ALDH), β-galactosidase (β-Gal)), reactive oxygen species (OCl^-, $ONOO^-$, $^{\bullet}OH$, $^1O_2$), human serum albumin (HSA), and bovine serum albumin (BSA), respectively, were shaken with 10 μM **Cy-ND** on a constant temperature shaker at 37 °C for 30 min, and the fluorescence intensity was measured by a fluorometer.

Toxicity Test of Cy-ND towards HepG2 、 Panc02-H7 and L02 Cells. 3-(4,5-dimethylthiazol-2-yl)-2,5-diphenyltetrazolium bromide (MTT) assays were carried out to evaluate the toxicity of **Cy-ND**. HepG2, Panc02-H7, and L02 cells were inoculated into 96 well plates with 5×10^3 cells per well and cultured at 37 °C and 5% CO_2 for 24 hours. After the cells completely adhered to the wall, various concentrations of **Cy-ND** were added, and cells were cultured for another 12 h. Then 100 μL MTT solutions (diluted to 0.5 mg/mL with DMEM) were added into each well. After 4 h, the MTT solution was removed, and 100 μL of DMSO was added to each well and shook for 10 minutes. Then the absorbance determined at 490 nm was operated on a reader. The relative cell viability (VR) was calculated as $VR = A/A_0 \times 100\%$, where A is the absorbance of the experimental group and A_0 is the control group. The cell viability of the control group was considered as 100%.

Measurement of Cell Fluorescence Intensity by High Content Screening Method. HepG2 cells were cultured in high-glucose Dulbecco's modified Eagle's medium (DMEM) supplemented with 10% fetal bovine serum and 1% penicillin and 1% streptomycin, and cells were cultured in an incubator with 5% CO_2 at 37 °C. Prior to imaging, HepG2 cells were cultured in 96 well plates with 5×10^3 cells per well with lipopolysaccharide, nystatin, oleic acid, ethanol, and dexamethasone for the various treatments. The cells were incubated with probe

Cy-ND (5 μM) and Hoechst 33342 (5 μM) for 30 min at 37 °C and then washed three times with PBS before imaging. Fluorescence images were captured with a 40× lens, relative fluorescence intensity changes before and after various physiopathological treatments were measured using the CellInsight CX7 LZR High Content Screening (HCS) platform (Thermo Fisher Scientific, Waltham, MA, USA).

Hepatic Ischemia-reperfusion Injury Model. Hepatic ischemia-reperfusion injury (HIRI) cell models were established by oxygen-glucose-serum deprivation/reperfusion. HepG2 cells were cultured in DMEM (without glucose and serum) and deoxygenated sodium dithionite (0.5 mM) for 30 min. Subsequently, these cells were incubated with high glucose and serum DMEM (standard DMEM) in a 5 % CO_2 and 95 % O_2 atmosphere for 30 min. Hepatic ischemia-reperfusion cells with different ischemia times were also designed by using the above ischemia incubation times of 2, 12 and 24 h, and then cells were incubated with standard medium for another 30 min, and the fluorescence intensity changes before and after the various treatments were observed by adding the **Cy-ND** (5 μM) and the Hoechst 33342 (5 μM). The cell culture medium of each group was removed, and all cells were washed with 100 μL of PBS three times before fluorescence imaging. Relative fluorescence intensity changes before and after treatments were measured using the CellInsight CX7 LZR High Content Screening (HCS) platform (Thermo Fisher Scientific, Waltham, MA, USA).

Acute Alcoholic Liver Injury Mouse Model. Twelve male mice of Kunming, with age 10 weeks and weight 17-20 g, were purchased from the Experimental Center of Shandong Second Medical University and kept in the pharmacology SPF animal room of Shandong Second Medical University. After 7 days of adaptive feeding, 12 Kunming mice were randomly divided

into 2 groups, 6 mice were randomly selected as the control group and 6 mice as the acute alcoholic liver injury (AALI) model group. The groups were treated as follows: control group: untreated mice group; AALI group: mice were orally administered with Chinese liquor (20 μL/g) at 8:30 am and 8:30 pm for 3 consecutive days. The Chinese liquor contained 52% alcohol by volume as ethanol. Prior to imaging, mice were injected with 100 μM **Cy-ND** via the tail vein and images were collected 30 min later.

Fluorescence Imaging of Mouse Models and Major organ. Mice were injected with the probe **Cy-ND** (100 μL, 100 μM) in the tail vein for 30 min, followed by fluorescence imaging using the IVIS Spectrum *in vivo* fluorescence imaging system. After anesthesia, the heart, liver, spleen, lung, and kidney were extracted, and washed with PBS (pH 7.4), and images of organ distribution were analyzed. The excitation wavelength was 766 nm and the emission wavelength was 806 nm.

H&E Staining. The mice in the AALI group and control group were sacrificed and dissected to isolate the liver, spleen, lung, heart and kidney. All isolated organs were fixed in 10 % paraformaldehyde for tissue staining. The samples were dehydrated, embedded, sectioned and stained by hematoxylin and eosin.

2. Synthesis of Cy-ND

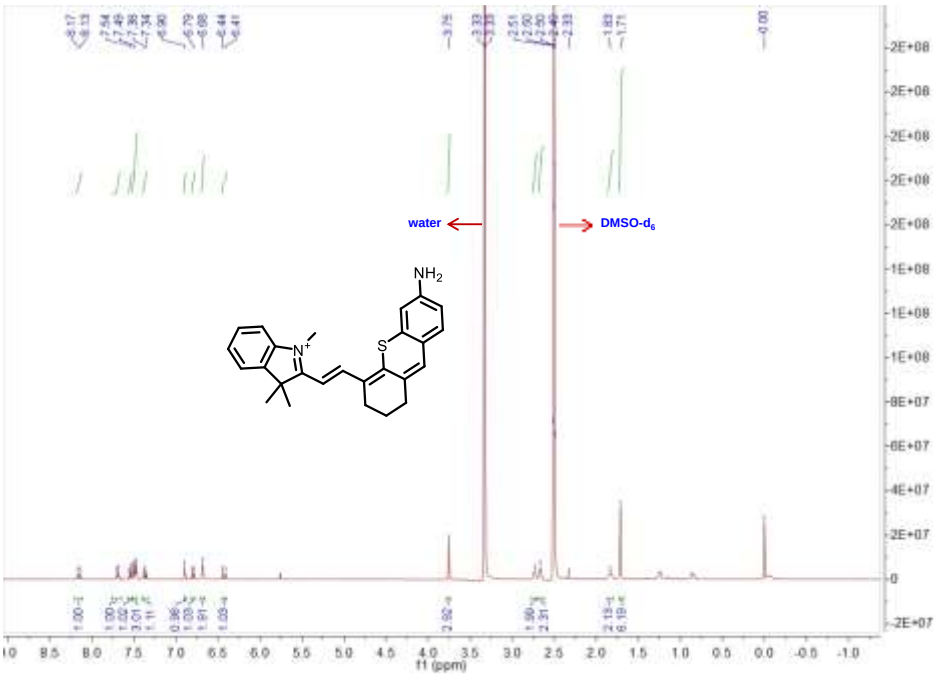

Fig. S1. ^{1}H NMR spectrum of **Cy-NH$_2$** (400 MHz, DMSO-*d*$_6$, 298 K).

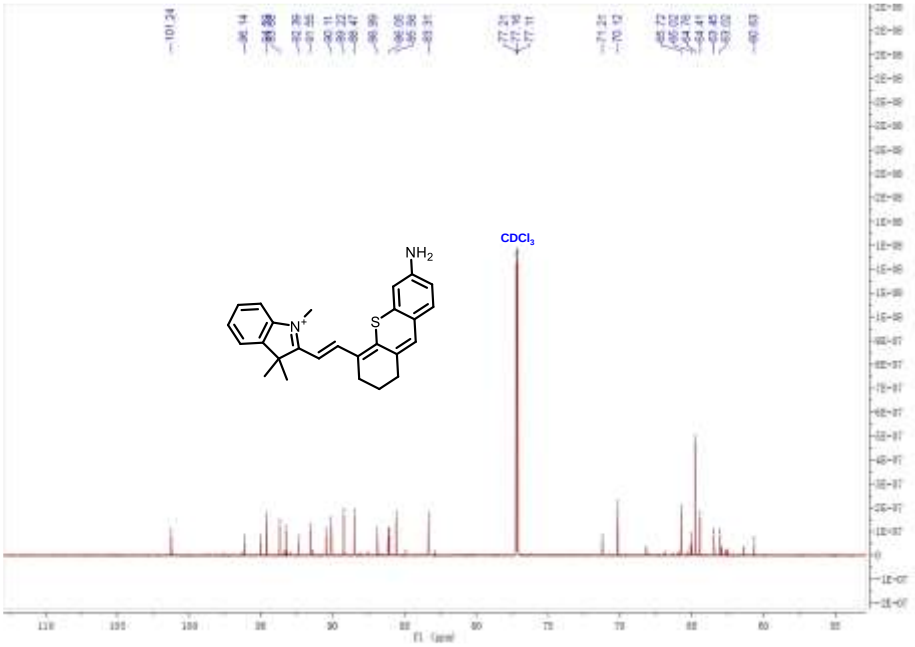

Fig. S2. ^{13}C NMR spectrum of **Cy-NH$_2$** (125 MHz, $CDCl_3$, 298 K).

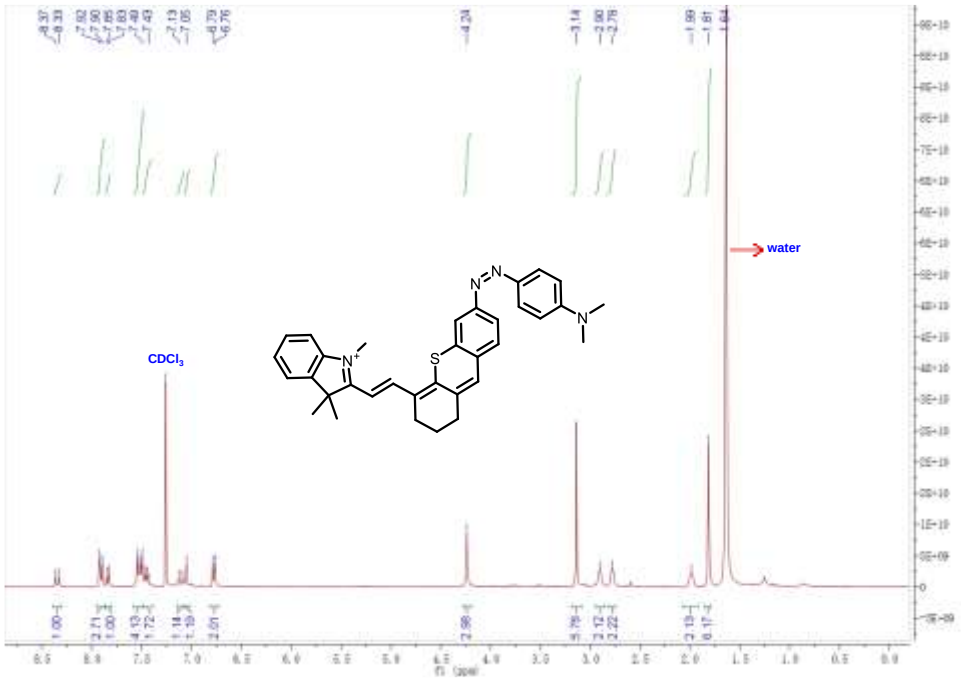

Fig. S3. ^{1}H NMR spectra of **Cy-ND** (400 MHz, $CDCl_3$, 298 K).

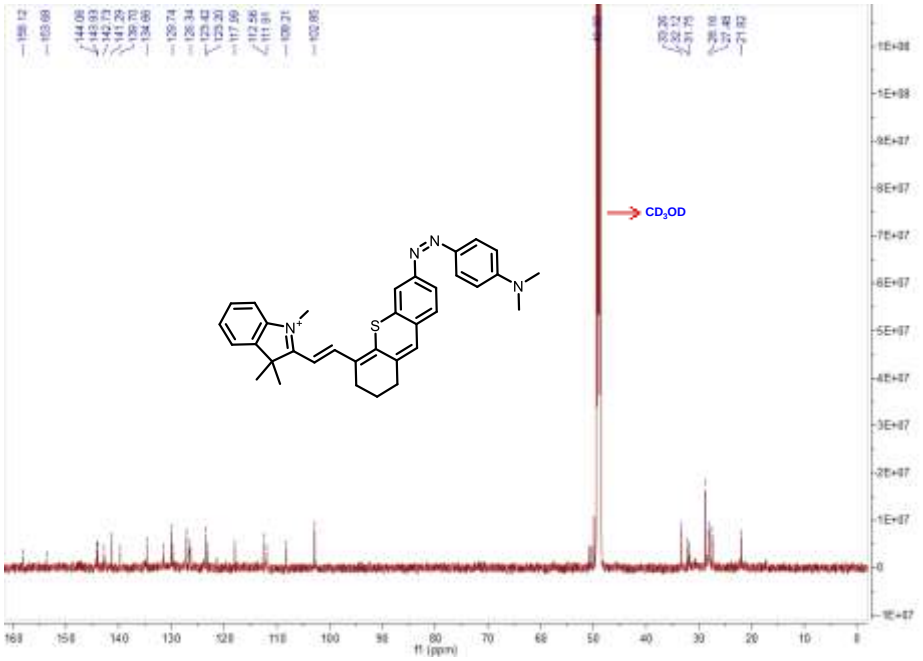

Fig. S4. ^{13}C NMR spectra of **Cy-ND** (125 MHz, CD_3OD, 298 K).

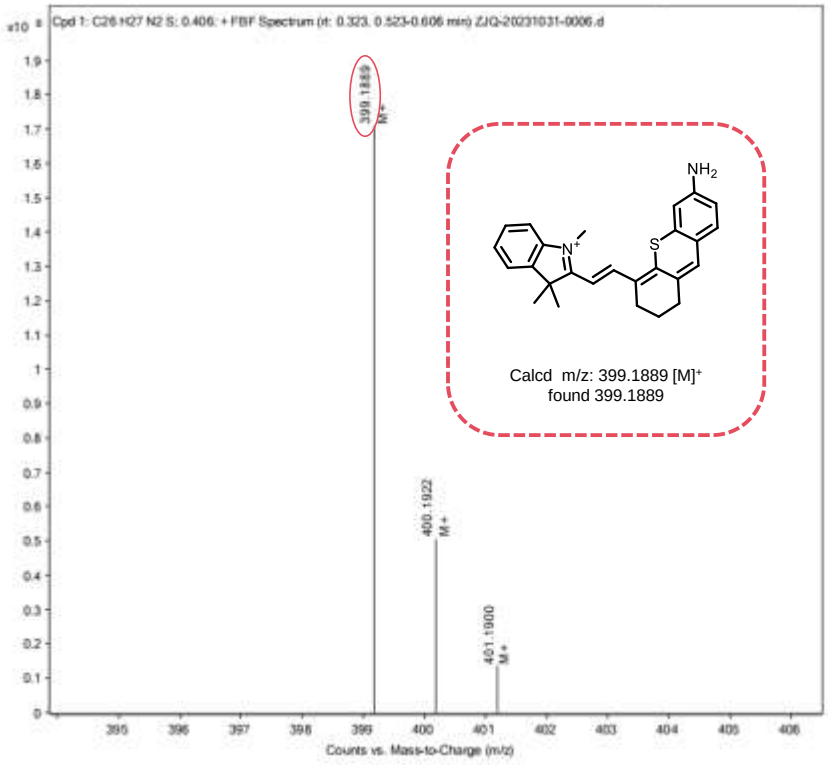

Fig. S5. HR-MS spectrum of **Cy-NH2**.

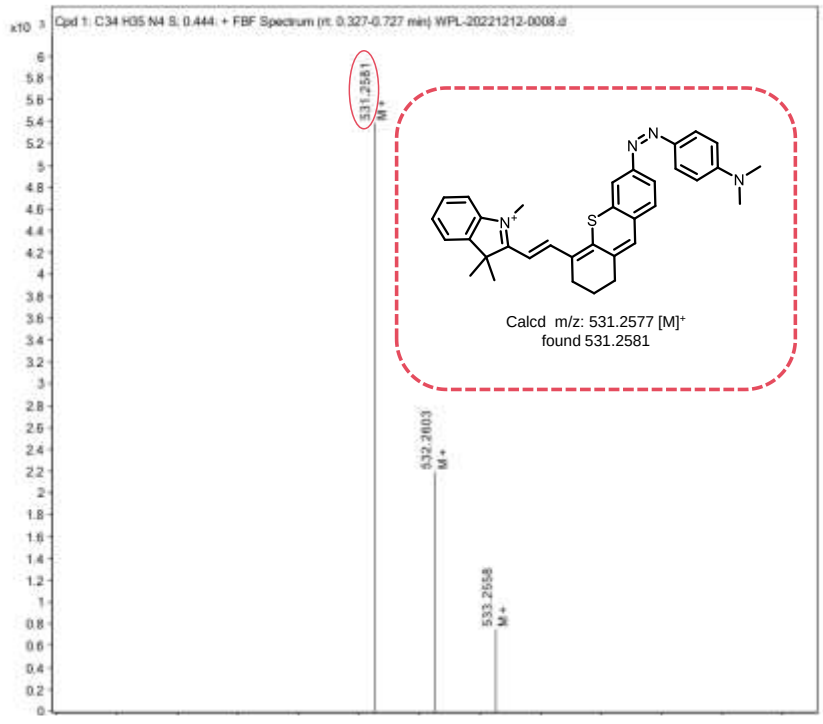

Fig. S6. HR-MS spectrum of **Cy-ND**.

3. Optimization of Experimental Conditions

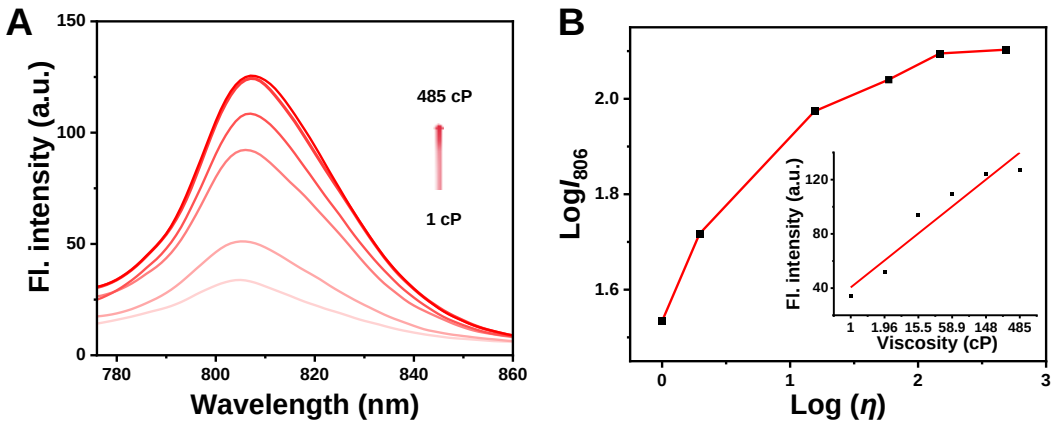

Fig. S7. (A) Fluorescence spectra of **Cy-ND** (10 μM) in sucrose solutions of different viscosities (as described in Table S1). (B) The linear relationship of **Cy-ND** (10 μM) between log I_{806} and log η. (Inset of B) Linear relationship between viscosity (cP) and fluorescence intensity. $\lambda_{ex/em}$ = 766/806 nm.

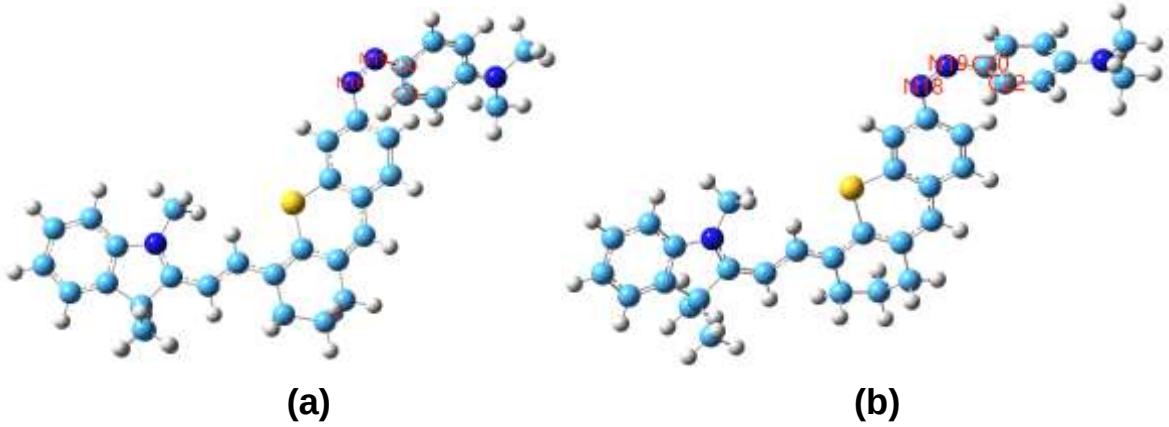

Fig. S8. The optimized geometry of **Cy-ND** in the ground state (S_0) (a), in the excited state (S_1) (b) in water using Gaussian 16 program by IEFPCM/B3LYP-D3(BJ)/6-31G(d) methods. Atom color coding: C, shallow blue; H, gray; S, yellow; N, dark blue.

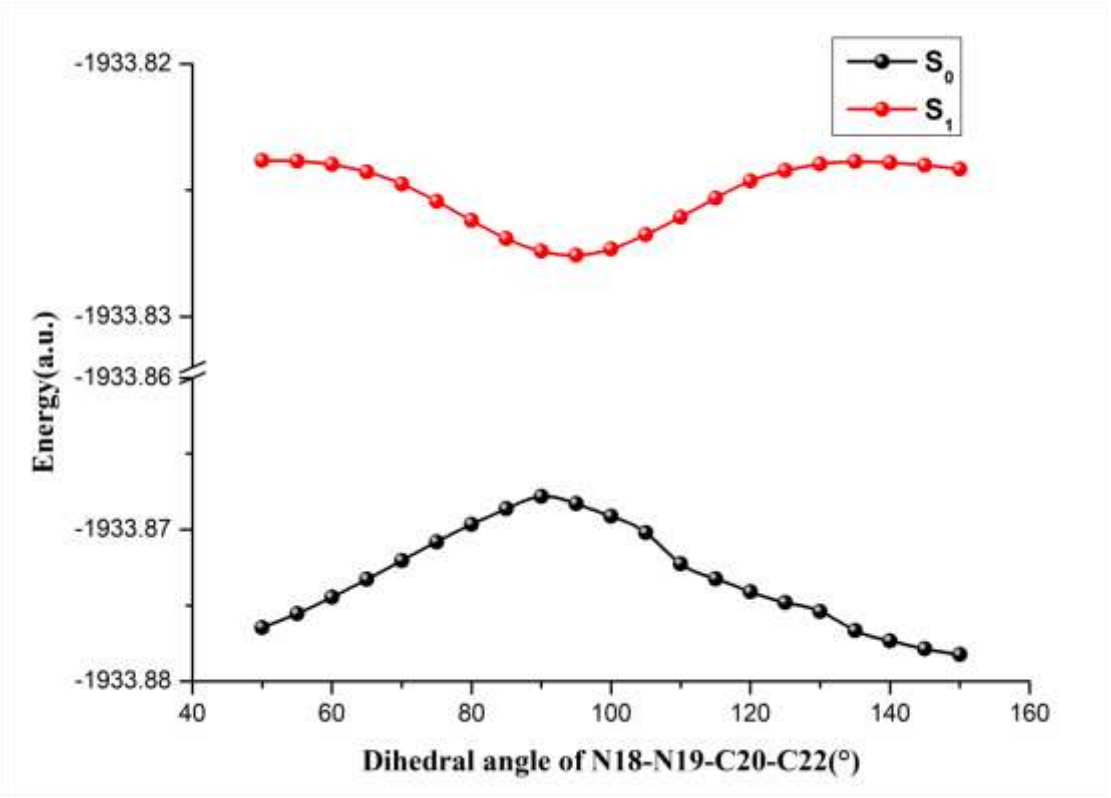

Fig. S9. The potential energy curves for **Cy-ND** along with the dihedral angle of N18-N19-C20-C22 in the S_0 and S_1 states in water.

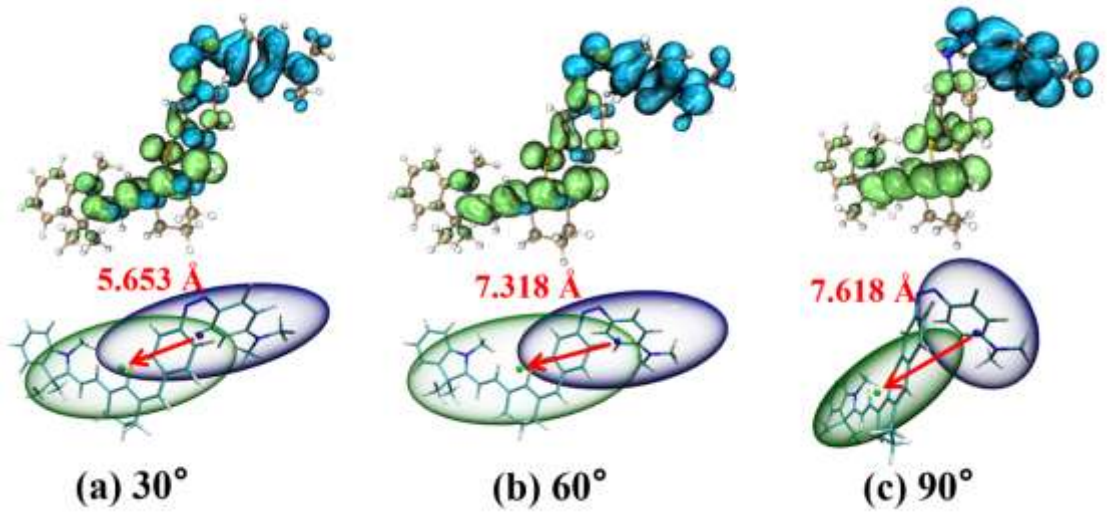

Fig. S10. The hole-electron distribution (on the top) and the C_{hole}-C_{ele} function diagrams (on the bottom) of **Cy-ND** with the dihedral angle of N18-N19-C20-C22 at 30° (a), 60° (b), 90°(c). (Blue: hole; Green: electron)

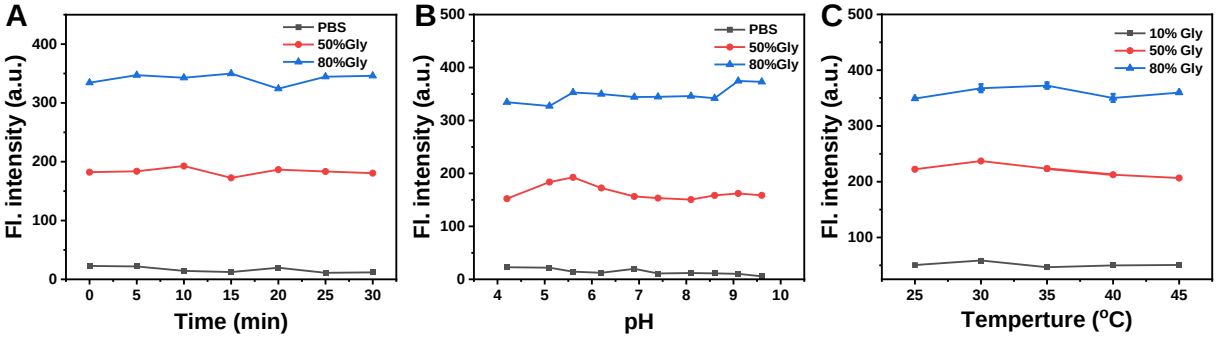

Fig. S11. The effects of (A) reaction time, (B) pH and (C) temperature on the fluorescence intensity of probe **Cy-ND** (10 μM) in the presence of varied glycerol volumetric ratios. $\lambda_{ex/em}$ = 766/806 nm.

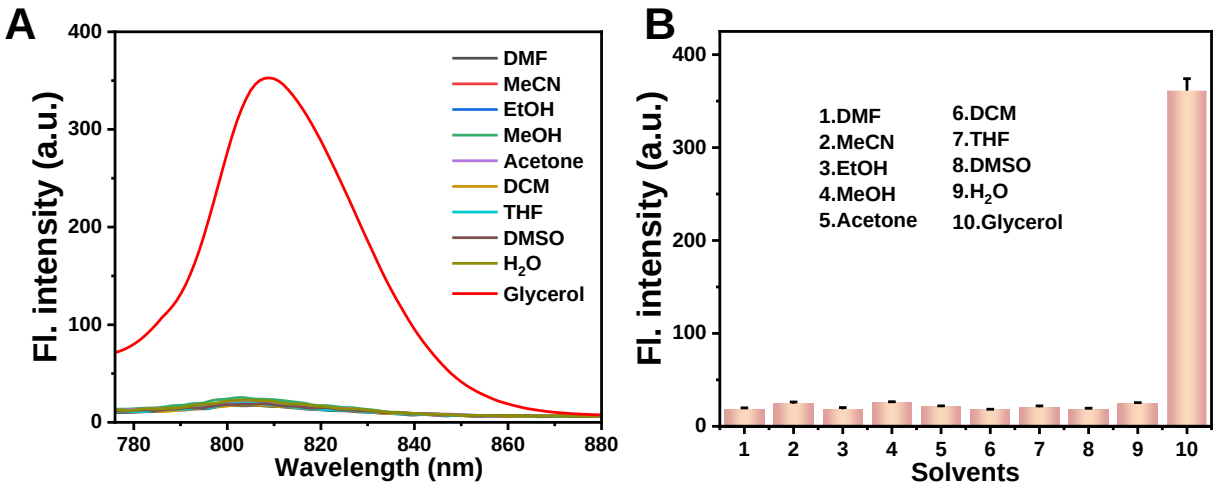

Fig. S12. The fluorescence responses (A) and histograms (B) of **Cy-ND** (10 μM) in different solvents: 1. DMF; 2. EtOH; 3. MeCN; 4. MeOH; 5. Acetone; 6. DCM; 7. THF; 8. DMSO; 9. H_2O; 10. Glycerol (containing 20% water). $\lambda_{ex/em}$= 766/806 nm.

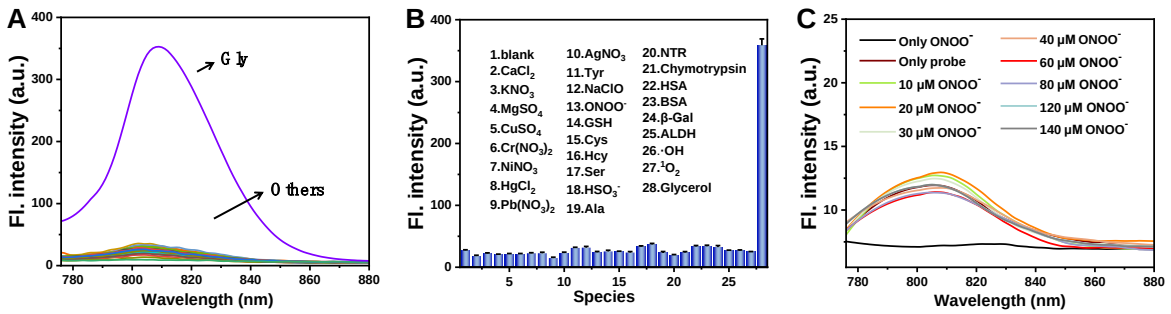

Fig. S13. The fluorescence responses (A) and histograms (B) of **Cy-ND** (10 μM) toward other biologically relevant species in pH 7.4 phosphate buffer: 1. blank, 2. Ca^{2+} (100 μM), 3. K^+ (100 μM), 4. Mg^{2+} (100 μM), 5. Cu^{2+} (100 μM), 6. Cr^{3+} (100 μM), 7. Ni^+ (100 μM) , 8. Hg^{2+} (100 μM), 9. Pb^{2+} (100 μM), 10. Ag^+ (100 μM), 11. Tyrosinase (5 U/mL), 12. NaClO (10 μM), 13. $ONOO^-$ (10 μM), 14. GSH (10 μM), 15. Cys (10 μM), 16. Hcy (10 μM), 17. Ser (100 μM), 18. HSO_3^- (10 μM), 19. Ala (10 μM), 20. NTR (5 μg/mL), 21. Chymotrypsin (100 μg/mL), 22. HSA

(10 μg/mL), 23. BSA (10 μg/mL), 24. β-Gal (4 U /mL), 25. ALDH (10 U/mL), 26. $^{\bullet}OH$ (10 μM), 27. $^1O_2$ (10 μM), 28. Glycerol (containing 20% water). (C) Fluorescence test of **Cy-ND** (10 μM) in different concentrations of $ONOO^-$ solution. $\lambda_{ex/em}$ = 766/806 nm.

4. Imaging Experiments of Cells

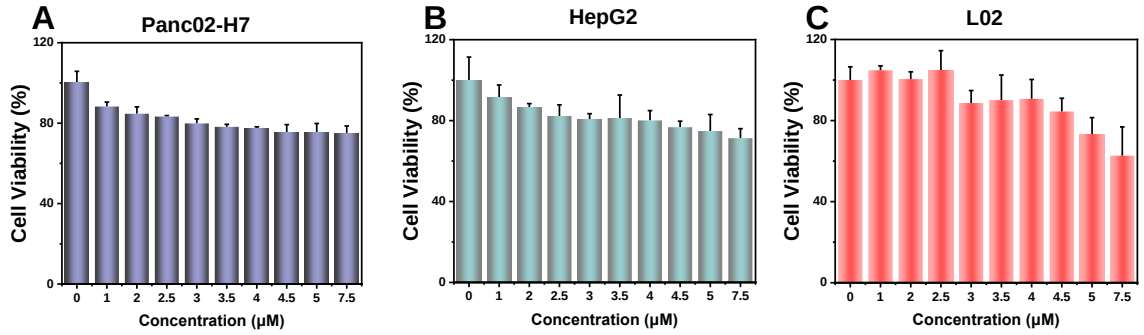

Fig. S14. The viability of Panc02-H7 (A), HepG2 (B) and L02 (C) cells incubated with different concentrations (0-7.5 μM) of **Cy-ND** for 12 h at 37 ℃. The cell viability was determined by standard MTT method, and the viability in the absence of **Cy-ND** was defined as 100%. The results are presented as mean ± standard deviation (n = 6).

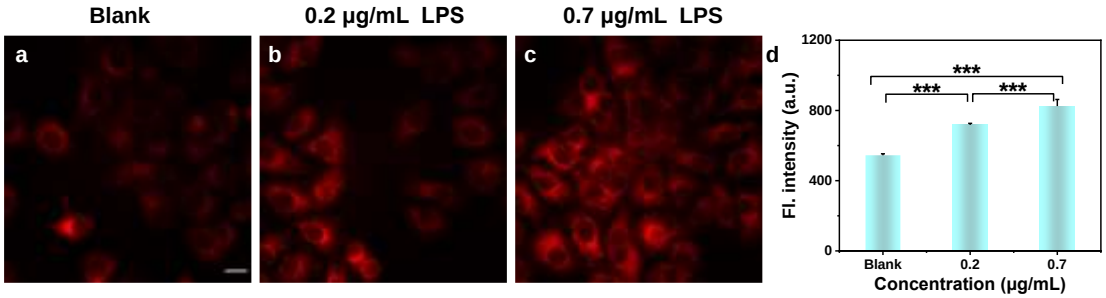

Fig. S15. Fluorescence images of **Cy-ND** (5 μM) in HepG2 cells induced by LPS ((a) blank, (b) 0.2 μg/mL, (c) 0.7 μg/mL) for 12 h. (d) The concentration-dependent mean fluorescence intensity, and analyzed with CellInsight CX7 LZR High-Content Screening (HCS) Platform, ***P < 0.001, Scale bar: 20 μm.

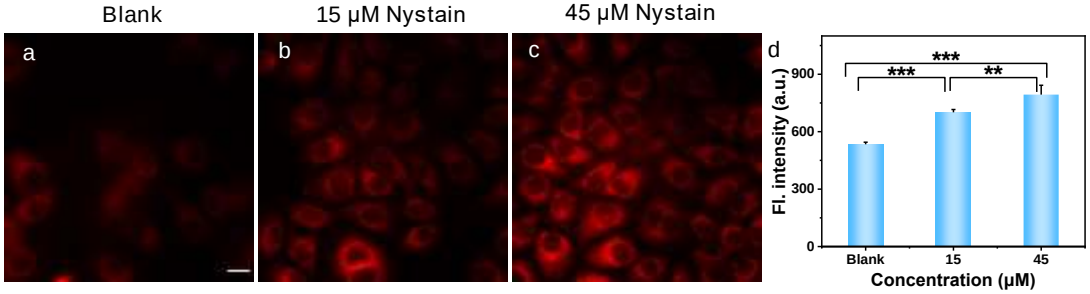

Fig. S16. Fluorescence imaging of cell viscosity in HepG2 cells induced by nystatin ((a) blank, (b) 15 μM, (c) 45 μM) for 30 min. (d) Comparison of red channel fluorescence intensities, and

analyzed with CellInsight CX7 LZR High-Content Screening (HCS) Platform, ***P < 0.001, **P < 0.01, Scale bar: 20 μm.

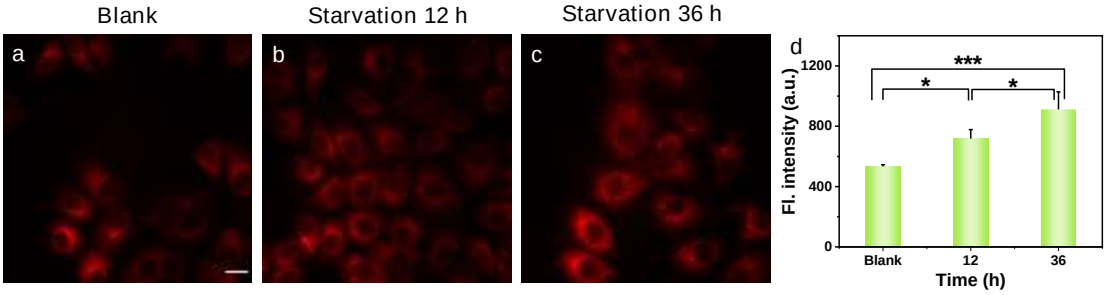

Fig. S17. Fluorescence imaging of **Cy-ND** (5 μM) in HepG2 cells cultured under starvation conditions. Mean fluorescence intensity changes of **Cy-ND** over time. (a) untreated, probe only added (b) starved for 12h, (c) starved for 36h. (d) Analyzed with CellInsight CX7 LZR High-Content Screening (HCS) Platform， ***P < 0.001, *P < 0.05, Scale bar: 20 μm.

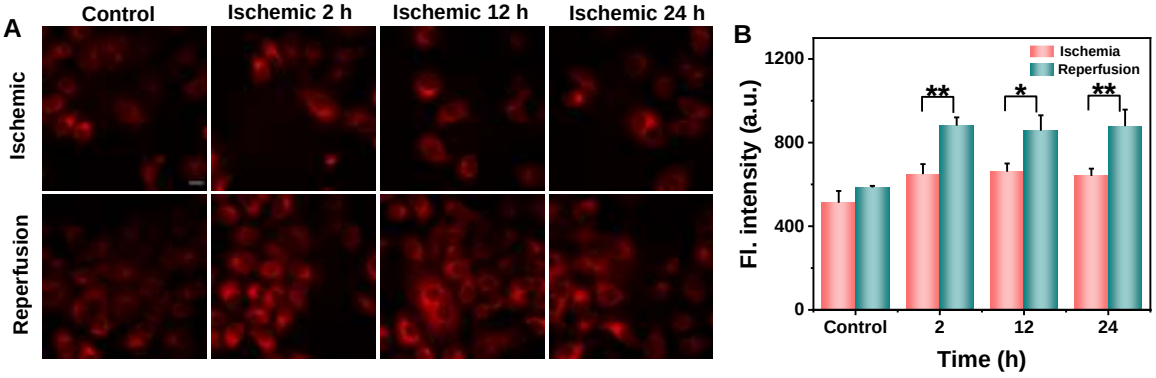

Fig. S18. HepG2 cells throughout HIRI. (A) Fluorescence imaging of **Cy-ND** (5 μM) hepatocytes subjected to 0, 2, 12 or 24 h ischemia and reperfusion for 30 min, and (B) analyzed using the CellInsight CX7 LZR high content screening (HCS) platform. Data are expressed as mean ± standard deviation. **P < 0.01, *P < 0.05, Scale bar: 20 μm.

5. Imaging Experiments of Animal

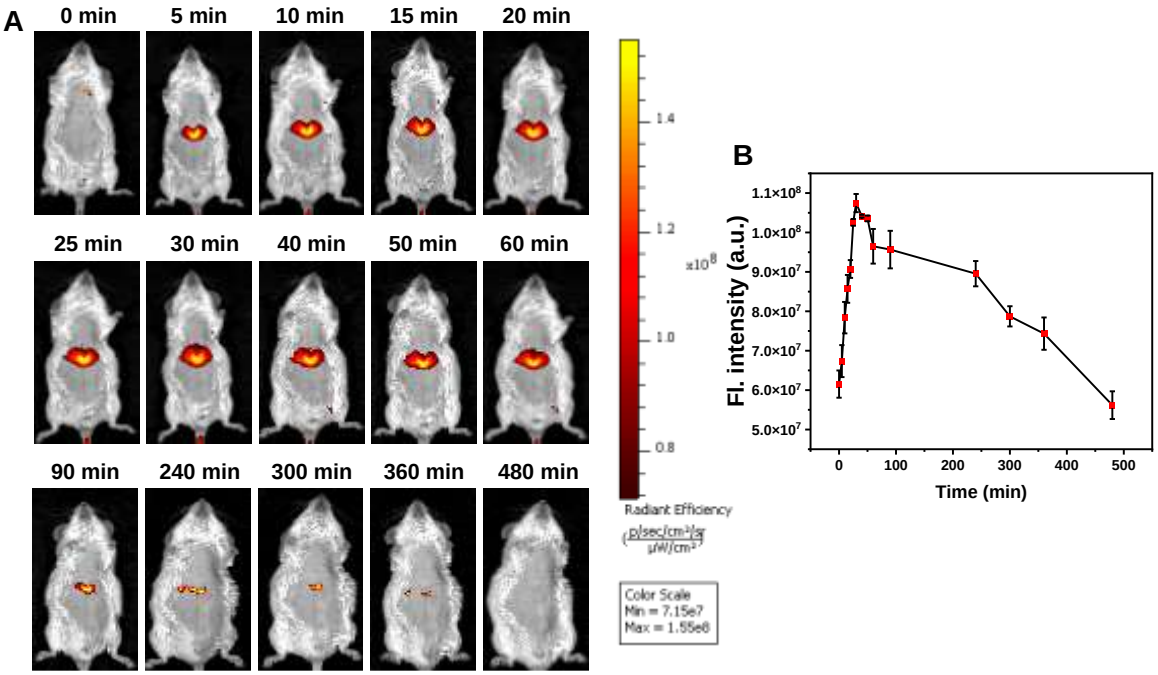

Fig. S19. (A) Real-time imaging of AALI mice after intravenous injection with **Cy-ND** (100 μM, 0.1 mL). (B) Corresponding fluorescence intensity of AALI mice after intravenous injection with **Cy-ND** for 0-480 minutes. λ_{ex} = 766 nm, and λ_{em} = 806 nm.

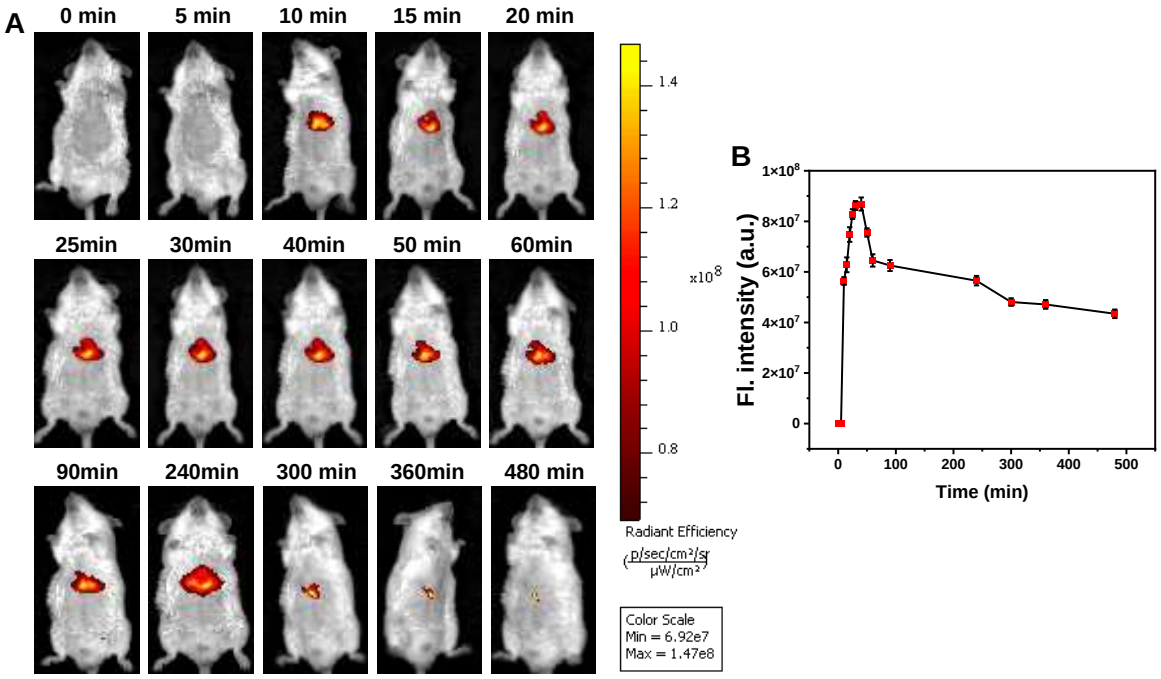

Fig. S20. (A) Real-time imaging of control mice after intravenous injection with **Cy-ND** (100 μM, 0.1 mL). (B) Corresponding fluorescence intensity of control mice after intravenous injection with **Cy-ND** for 0-480 minutes. λ_{ex} = 766 nm, and λ_{em} = 806 nm.

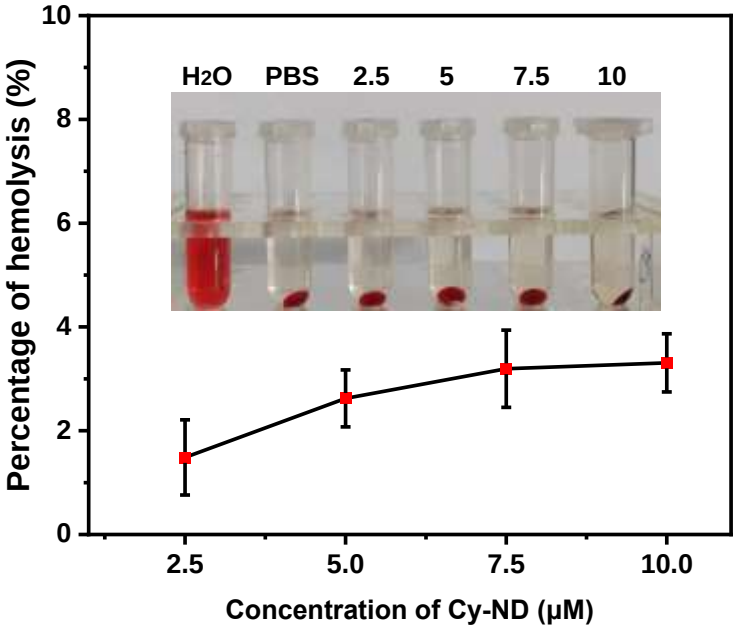

Fig. S21. Hemolysis test with **Cy-ND** (2.5-10 μM, dissolved in PBS) at room temperature. Pure water and PBS were used the control. The inset is the photographs of the hemolysis experiment. The hemolysis rate increased slightly with the increased concentration of **Cy-ND**, but remained low (3.3%) at 10 μM.

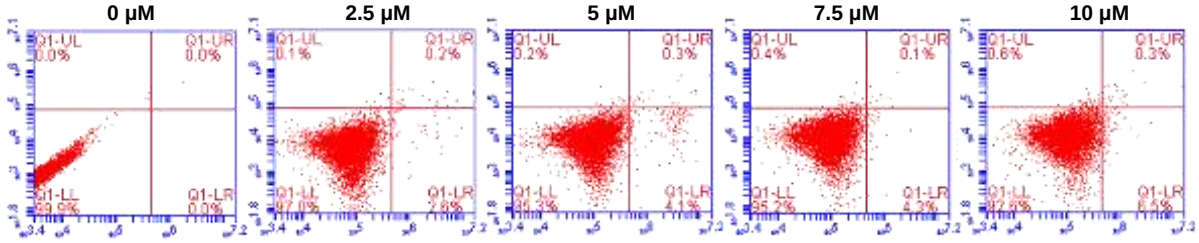

Fig. S22. L02 cells treated with PBS (control), various concentration of **Cy-ND** (2.5-10 μM) for 30 min, were analyzed by flow cytometry with FITC- Annexin V/PI double staining, Q1-UL, Q1-UR, Q1-LR, and Q1-LL represent the regions of dead cells, late apoptotic cells, early apoptotic cells, and normal cells, respectively. The results demonstrated that the probe had good biosafety, and could be applied in biological experiments.

6. Additional Tables

Table S1. The viscosity of sucrose solutions at different concentrations at 20 °C. [5]

Sucrose concentration (g/100g water)	Viscosity (cP)
0	1
20	1.96
50	15.5
60	58. 9
65	148
70	485

Atomic coordinate information is given below.

Table S2. Ground State Standard orientation:

Atomic	X	Y	Z
C	1.41861700	4.45358200	-0.41029400
C	0.43531300	4.28678100	0.74648300
C	-0.14306600	2.88800000	0.75939200
C	0.72617600	1.81548600	0.36596900
C	2.07189100	2.03434800	0.00997200
C	2.55835600	3.44669500	-0.26486500
C	-1.42711200	2.69056000	1.19548100
C	-1.48068300	0.21793300	0.99381700
C	-2.09558200	1.43879700	1.35498100
C	-3.39853500	1.38215300	1.90717600
H	-3.87327400	2.31071800	2.20994400
C	-4.06348700	0.18567500	2.06211700
C	-3.43747600	-1.02239400	1.67521700
C	-2.13492100	-1.00247700	1.17489000
H	-1.99137000	3.57188300	1.48994600
H	-5.06263700	0.15870800	2.48167300
H	-1.65098200	-1.93854700	0.91495300
N	-4.02213600	-2.27976600	1.97649700
N	-5.19569500	-2.60702000	1.64276000
C	-5.98226200	-1.91171200	0.70989400
C	-7.36954600	-2.13174800	0.82058900

C	-5.52070400	-1.13439200	-0.37608400
C	-8.27049800	-1.53439800	-0.03841500
H	-7.72395700	-2.77066800	1.62366400
C	-6.40804600	-0.56633500	-1.26702300
H	-4.45971500	-1.00794600	-0.54950700
C	-7.81553400	-0.71802600	-1.10967900
H	-9.32869400	-1.70990800	0.10450500
H	-6.01332300	-0.00473300	-2.10375100
N	-8.69030300	-0.12066300	-1.96887500
C	-10.12383700	-0.33795200	-1.82298800
H	-10.47895800	0.00020200	-0.84208000
H	-10.64919300	0.22982800	-2.58995000
H	-10.38493900	-1.39754400	-1.93835500
C	-8.19798800	0.68711100	-3.07749900
H	-9.04734200	1.10759600	-3.61458400
H	-7.57587200	1.51536700	-2.71858500
H	-7.60563800	0.08977400	-3.78250400
S	0.10445900	0.17339200	0.24010000
C	2.97560800	0.95981700	-0.06034100
H	2.60371300	-0.00601400	0.25455200
C	4.32167600	1.06738800	-0.39627800
H	4.71066000	2.05381300	-0.62028000
C	6.38864500	-1.94032000	-0.32387800
C	7.40749600	-0.98964600	-0.42367800
C	8.73345200	-1.39466500	-0.43845000
C	9.01920300	-2.76351100	-0.34247200
C	7.98720200	-3.70036600	-0.23362600
C	6.64523200	-3.30294500	-0.22110300
C	5.29502400	0.06256800	-0.40747900
C	6.78794600	0.38772300	-0.50570200
H	9.53683600	-0.66873400	-0.52060300
H	10.05148200	-3.09865400	-0.34890800
H	8.22471500	-4.75641400	-0.15350100
H	5.85387700	-4.03721100	-0.12455100
N	5.13469200	-1.27499000	-0.34673400
C	7.23008200	1.28453500	0.66980900
H	6.73062000	2.25694800	0.62569800
H	6.99797000	0.81512200	1.63009500
H	8.31026600	1.45066600	0.61676300
C	3.87087000	-1.99856200	-0.39494600
H	3.39493300	-2.03022100	0.58985000
H	3.20540600	-1.51405700	-1.11189000
H	4.06171200	-3.01631600	-0.73126900
C	7.10404300	1.06720200	-1.85729200
H	6.77539000	0.44639400	-2.69564300

H	6.61353100	2.04263100	-1.92827800
H	8.18418200	1.22047400	-1.94113300
H	0.96017500	4.46887000	1.69537000
H	-0.37986600	5.01446100	0.68946600
H	1.82003600	5.47123200	-0.42929900
H	0.89459400	4.28969400	-1.36002200
H	3.22909100	3.76146700	0.54731700
H	3.16399500	3.44250100	-1.17842700

Excited State Standard orientation:

Atomic	X	Y	Z
C	1.89904900	4.53455500	-0.40511600
C	0.59124700	4.25372800	0.33145900
C	0.06792100	2.87147600	-0.00250400
C	1.01114900	1.85409400	-0.24446700
C	2.41826300	2.05903600	-0.15288000
C	2.94095400	3.48134700	-0.03186400
C	-1.31052600	2.66913700	-0.00627600
C	-1.26729500	0.22608400	-0.44152000
C	-1.97271000	1.43524100	-0.16493100
C	-3.38872600	1.34367900	-0.02387600
H	-3.94040900	2.25602900	0.18304200
C	-4.06180700	0.15236100	-0.13404000
C	-3.34055700	-1.04688700	-0.39226300
C	-1.93414900	-0.97911900	-0.53878600
H	-1.93751500	3.53402000	0.19280000
H	-5.13635600	0.14623800	-0.01816600
H	-1.39905000	-1.90199400	-0.73842600
N	-3.86336200	-2.32297200	-0.52167300
N	-5.07898700	-2.60850800	-0.41835700
C	-6.24173000	-1.92690500	-0.17735100
C	-6.75317700	-1.83123300	1.14530000
C	-7.04217000	-1.47108400	-1.25988500
C	-7.96358800	-1.23204600	1.38255700
H	-6.15848900	-2.21420300	1.96647800
C	-8.25273900	-0.87054900	-1.02662300
H	-6.66826300	-1.58086600	-2.27120000
C	-8.75504900	-0.72295800	0.30488800
H	-8.31150000	-1.14277700	2.40243500
H	-8.82555900	-0.50516800	-1.86779000
N	-9.94477000	-0.12347300	0.53788000
C	-10.46286600	0.00433800	1.90189100
H	-9.77709200	0.59082900	2.52021900
H	-11.42343900	0.51275700	1.86740000

H	-10.60289400	-0.98127600	2.35503400
C	-10.74899900	0.39790600	-0.56965400
H	-11.64234200	0.86800900	-0.16533000
H	-10.18486700	1.14523400	-1.13475300
H	-11.05010600	-0.41060200	-1.24235300
S	0.47155800	0.24044700	-0.77122200
C	3.30278500	0.98657700	-0.14447900
H	2.86758800	-0.00360800	-0.15207000
C	4.70666400	1.08808600	-0.03070000
H	5.12313600	2.08272900	0.08549200
C	6.71326600	-1.94927500	0.02592500
C	7.71516600	-1.02967300	0.35505800
C	9.00532100	-1.46709000	0.60927100
C	9.28220900	-2.84053900	0.53846500
C	8.26975700	-3.74786800	0.21724600
C	6.96262400	-3.31693800	-0.04319200
C	5.65268000	0.08302800	0.01959400
C	7.12431700	0.36502400	0.35732400
H	9.79056800	-0.75998000	0.86157500
H	10.28693100	-3.19962000	0.73824500
H	8.49244300	-4.80965900	0.17158800
H	6.18422300	-4.03426500	-0.27770200
N	5.50235200	-1.26005000	-0.19947700
C	7.25688200	1.03154500	1.74112300
H	6.77850500	2.01592000	1.74566400
H	6.79226300	0.41637900	2.51750700
H	8.31474500	1.16315200	1.99075200
C	4.31091900	-1.91725100	-0.71070700
H	3.57393100	-2.09218600	0.08026200
H	3.86282100	-1.30204100	-1.49397100
H	4.59405800	-2.87515500	-1.14631900
C	7.77249400	1.24804400	-0.73073500
H	7.67556400	0.78671800	-1.71806400
H	7.30219500	2.23606300	-0.76012300
H	8.83733300	1.38125300	-0.51385600
H	0.76153300	4.32792500	1.41558800
H	-0.17288800	4.99752400	0.08269200
H	2.27214100	5.53390000	-0.15907600
H	1.71704700	4.50992600	-1.48690500
H	3.28172800	3.65444400	0.99953900
H	3.82498100	3.59698100	-0.66876500

Table S3. The hole-electron centroid distance (*D*), the hole-electron distribution values (S_r), the average width of the hole-electron distribution (*H*), the hole-electron separation degree (*t*), the hole delocalization index (*HDI*) and the electron delocalization index (*EDI*).

Dihedral angle of N18-N19-C20-C22	*D* (Å)	S_r	*H* (Å)	*t* (Å)	*HDI*	*EDI*
30°	5.653	0.52383	4.567	1.715	7.47	6.48
60°	7.318	0.39630	4.028	3.918	9.16	6.48
90°	7.618	0.14600	3.141	5.487	11.25	7.09

Supporting reference

[1] Z. Liu, T. Lu and Q. Chen, *Carbon*, 2020, **165**, 461-467.

[2] T. Lu and F. Chen, *J. Comput. Chem.*, 2011, **33**, 580-592.

[3] W. Humphrey, A. Dalke and K. Schulten, *J. Mol. Graph.*, 1996, **14**, 33-38.

[4] D. Xie, W. Ma, C. Wang, W. Zhang and Z. Ding, *Chem. Commun.*, 2023, **59**, 1030-1033.

[5] Honig, P. Principles of Sugar Technology; Elsevier Pub. Co., 1953. ISBN: 978-1-4832-3252-2.